262

SCR-70

MASTER

Sandia Corporation

REPRINT

VARIABLE INDUCTANCE MODULATION OF A TRANSISTORIZED SUBCARRIER OSCILLATOR

by

CE Land

MAY 1959

DISCLAIMER

SCR-70
TID 4500 (14th Ed.)
INSTRUMENTS

Presented at NATIONAL TELEMETERING CONFERENCE
Denver, May 1959

Printed in USA. Price $1.00. Available from the Office of Technical Services, Department of Commerce, Washington, D.C.

VARIABLE INDUCTANCE MODULATION OF A TRANSISTORIZED SUBCARRIER OSCILLATOR

C. E. Land
Staff Member
Instrumentation Development Department
Sandia Corporation

SUMMARY

When a ferrite material is subjected to the influence of both a-c and d-c fields, the inductance of a coil wound on the ferrite material depends upon the magnitudes of both the a-c and the d-c fields. If a ferrite-cored inductor is used in the frequency determining circuit of an oscillator, the inductance, and, hence, the oscillator frequency can be varied by changing the magnitude of the field acting on the ferrite core material. Variable inductance modulation results when this principle is applied to produce frequency modulation of an oscillator.

The use of the variable inductance modulator has given rise to new concepts of simplicity, flexibility, and reliability in telemetry subcarrier oscillator design. A modulator of this type has been developed for use with a transistor oscillator to form the nucleus of a complete line of FM/FM subcarrier oscillators.

The design of a variable inductance modulated oscillator requires consideration of certain aspects of the fundamentals of both the oscillator circuit and the magnetic circuit. This paper presents one method of approach leading to the design of such an oscillator. It is hoped that the advantages of variable inductance modulation, especially in the field of FM/FM subcarrier oscillator design, will bring about the development of new and better design methods in the near future.

INTRODUCTION

Most transducers (strain gages, resistance bridge transducers, voltage transducers, thermocouples, etc.) commonly used in aircraft and missile telemetering systems convert the magnitude of the sensed phenomena into a voltage or current of proportional magnitude. The role of the subcarrier oscillator in the FM/FM telemetering system is to convert the voltage or current outputs of these transducers into frequency modulated signals. This conversion process is a potential source of error in the system. Many of the design requirements imposed on subcarrier oscillators are directly related to minimizing this error. Of equal importance in missile telemetry are the restrictions on size, weight and power consumption, since these factors limit the number of telemetry channels available for any particular test. In addition, the subcarrier oscillator must operate normally while exposed to increasingly severe missile environmental conditions. Since all the above factors must be given due consideration in subcarrier oscillator design, a reasonable approach to the ideal subcarrier oscillator poses formidable problems. 1

While seeking a solution to subcarrier oscillator design problems involving the requirements indicated above, it became necessary to investigate the principles and characteristics of variable inductance modulation. During the early stages of this investigation, the transistor oscillator circuit (Figure 1) was developed. 2 The feasibility of applying the variable inductance modulation principle to this circuit was almost immediately apparent. Considerable developmental effort was then directed toward producing a practical variable inductance modulated subcarrier oscillator based on this circuit. This paper describes the circuit which resulted from these efforts. The variable inductance modulator makes use of the fact that the inductance of a coil wound on a core depends upon the permeability of the core material. The term "permeability" is, in general, used to define the relationship between the magnetic induction or flux produced by a given magnetizing force, and the magnitude or intensity of that particular magnetizing force. The permeability of a ferromagnetic or ferrimagnetic (ferrite) material is greater than unity. Furthermore, the permeability of such material (generally designated a "magnetic" material) depends upon the magnetic field strength, the previous magnetic history, temperature and physical stresses in the material. 3,4 If all the factors affecting permeability of the core material are controlled in a predetermined manner, the inductance of a coil wound on the core material is similarly controlled. This principle has been applied to the design of the variable inductance modulator.

The scope of this paper is limited to an analysis of a basic variable inductance modulated oscillator. The transistor oscillator and the modulator are first described separately, followed by an analysis of the combined modulator-oscillator circuit. Particular emphasis is placed upon linear correspondence between oscillator frequency and modulator input stimuli. One method of obtaining this linear operation is described. Other methods requiring further investigation of the magnetic circuit are possible. Temperature stability of the circuit is discussed briefly. Some particular applications of the circuit are presented to illustrate the inherent advantages of the circuit.

OSCILLATOR

Description

A simplified schematic of the oscillator is shown in Figure 1. The oscillator is essentially a series resonant circuit and a transistor switch. The coupling between the resonant circuit elements and the transistor consists of an RC phase shift-attenuator network. Since the circuit components in this network affect the oscillator frequency, they are treated in this analysis as part of the series resonant circuit.

The oscillator frequency is the natural frequency of this series resonant circuit. The transistor functions as a switch, exhibiting alternately high and low impedances during successive half cycles of operation. When the transistor impedance is high, energy is supplied to the series resonant circuit (charge half-cycle). When the transistor impedance is low, energy is supplied by the resonant circuit to the network (loss half-cycle). During the loss half-cycle, the battery current is limited by the load resistor, Rl. A more detailed description of the circuit appears in Reference 2.

Circuit Theory

The oscillator is frequency modulated by varying the impedance of the modulator coil connected in the oscillator series resonant circuit. An expression for the oscillator frequency as a function of this impedance will be derived below. An approximate equivalent circuit of the oscillator is shown in Figure 2. The transistor emitter, base, and collector resistances are represented by the symbols r_e, r_b, and r_c, respectively. A complete list of symbols is given in Appendix A. The instantaneous values of resistances, r_e, r_b, and r_c, are determined by the values of voltages, V_{BE} and V_{CE}, at any instant. The peak-to-peak amplitude of voltage, V_{BE}, is sufficiently high to cause the transistor to act as a switch. During large positive swings of V_{BE}, when the base is positive with respect to the emitter, the transistor is essentially cut off. It is during this part of the cycle that r_e, r_b, and r_c attain maximum values. When V_{BE} swings very far negative, i.e., the base becomes appreciably negative with respect to the emitter, the transistor is driven into saturation. It is during this part of the cycle that r_e, r_b, and r_c attain their minimum values. If the transistor were an ideal switch, the maximum and minimum values of r_e, r_b, and r_c would be infinity and zero, respectively. For the sake of simplifying this analysis, let us assume that the transistor approaches ideal switching action. With this assumption, theoretical limits can be calculated for the lumped R, L, and C of the resonant circuit. If the Q of the resonant circuit is sufficiently high (on the order of ten or greater), the theoretically ideal limits will enclose relatively small intervals of possible values of R, L, and C. This will permit approximation of these values with sufficient accuracy for this analysis.

The assumption of the ideal switch gives rise to two equivalent circuits representing the "off" and "on" switching states. These equivalent circuits are shown in Figures 3A and 3B. In the following analysis, the parameters which are common to both circuits, but have different values in the two circuits, will be denoted by the subscripts 1 and 2. The subscript, 1, refers to the "off" or nonconducting state of the transistor; the subscript, 2, refers to the "on" or conducting state of the transistor.

Consider first the "off" condition depicted by Figure 3A. The lumped resonant circuit resistance, R_1, consists of R1 (load resistance), R_L (the resistance contributed by the inductor), and R_c (the series equivalent resistance attributed to R2). The resonant circuit series inductance, L, is simply the inductance of the modulator output winding. The equivalent resonant circuit series capacitance, C_1, is the effective capacitance of the C1 and C2 combination.

$$R_1 \triangleq R1 + R_L + R_c \tag{1}$$

where:

$$R_c \triangleq \frac{R2\ C2^2}{R2^2\ {}_1^2\ C1^2\ C2^2 + (C1 + C2)^2} \tag{2}$$

$$C_1 \triangleq \frac{\omega_1^2\ C1^2\ C2^2\ R2^2 + (C1 + C2)^2}{\omega_1^2\ C1\ \ C2^2\ R2^2 + (C1 + C2)} \tag{3}$$

The expressions for R_c and C_1 are derived in Appendix B.

Figure 3B is the equivalent circuit for the "on" state. The resistance, R_2, is the effective series resistance of the inductor, R_L. Again, L is the resonant circuit series inductance which is the inductance of the modulator output winding. The effective resonant circuit series capacitance, C_2, is the sum of C1 and C2.

In an operating oscillator, R_1 and R_2 are the limiting values of R (the true equivalent series resonant circuit resistance).

$$R_2 < R < R_1 \tag{4}$$

In a similar sense, C_1 and C_2 are the limiting values of C (the true equivalent series resonant circuit capacitance).

$$C_1 < C < C_2 \tag{5}$$

The range of possible values of R and C for any given set of oscillator circuit components can be illustrated graphically by plotting the points S_1 and S_2 corresponding to the "off" and "on" conditions, respectively, in the complex frequency plane. A typical plot of this type is shown in Figure 4. The points S_1 and S_2 are defined as:

$$S_1 = -\alpha_1 \pm j\omega_1 \tag{6}$$

$$\alpha_1 = \frac{R_1}{2L} \tag{7}$$

$$\omega_1 = \left[\frac{1}{LC_1} - \frac{R_1^2}{4L^2}\right]^{\frac{1}{2}} \tag{8}$$

where: R_1 is defined by equation (1)

C_1 is defined by equation (3)

$$S_2 = -\alpha_2 \pm j\omega_2 \tag{9}$$

$$\alpha_2 = \frac{R_2}{2L} \tag{10}$$

$$\omega_2 = \left[\frac{1}{LC_2} - \frac{R_2^2}{4L^2}\right]^{\frac{1}{2}} \tag{11}$$

where: $R_2 = R_L$

$C_2 = C1 + C2$

Any unique set of values of R and C within the ranges given by Expressions (4) and (5) will result in a corresponding value of S which lies on a straight line joining S_1 and S_2. Therefore, there is a point S on the straight line joining S_1 and S_2 which corresponds to the true equivalent series resonant circuit R, L, and C and the true frequency, ω, of the oscillator.

$$S \triangleq -\alpha \pm j\omega \tag{12}$$

$$\alpha \triangleq \frac{R}{2L} \tag{13}$$

$$\omega \triangleq \left[\frac{1}{LC} - \frac{R^2}{4L^2}\right]^{\frac{1}{2}} \tag{14}$$

where: R, L, and C are the true equivalent series resonant circuit parameters of the oscillator

ω is the true oscillator operating frequency.

If the true oscillator frequency, ω, is measured, the imaginary component of S is determined. Since S is a point on the line joining S_1 and S_2, and $\omega_1 \neq \omega_2$, ω must belong to a unique point S. Therefore, if the point $S_K = j\omega$ is plotted on the ordinate, and a line parallel to the abscissa is constructed through S_K, the intersection of this line and the line joining S_1 and S_2 is the point $S = -\alpha + j\omega$. Since the inductance, L, of the oscillator series resonant circuit can be measured, R and C in the true equivalent series resonant circuit can be determined. From the definition of α (Equation (13)):

$$R = 2L\alpha \tag{15}$$

where: α is the graphically determined real component of S.

From Equation (14) it is possible to deduce the relationship:

$$|S|^2 = \frac{1}{LC} \tag{16}$$

The true value of C is then:

$$C = \frac{1}{|S|^2 L} \tag{17}$$

The actual oscillator frequency, ω , in terms of the true equivalent series resonant circuit R (Equation (15)), L, and C (Equation (17)) is expressed by Equation (14). When the oscillator is variable inductance modulated, both L and R depend upon the magnitude of the input signal. It is assumed, however, that C remains constant at all frequencies within the bandwidth of any particular oscillator. Equation (14) can then be expressed as:

$$\omega = \left[\frac{K}{L} - \frac{R^2}{4L^2}\right]^{\frac{1}{2}} \qquad \omega - \Delta\omega \leq \omega \leq \omega \quad \Delta\omega \tag{18}$$

where: K is equal to the constant $\frac{1}{C}$

$\Delta\omega$ is 7.5% ω for all standard telemetry channels; 15% ω for special wide bandwidth channels.

MODULATOR

Description

The variable inductance modulator consists of three or four coils wound on two matched toroidal cores. The core material is a ferrite which belongs to the class of materials designated ferrimagnetic. A generalized configuration of the modulator is shown in Figure 5. This figure is drawn so that the modulator windings include one or more input or signal windings, a bias winding and an output winding. It is the output winding which is connected in the series resonant circuit of the oscillator. In actual operation the output winding is the series-connected combination of two windings, one on each core. These windings are first wound on the cores; the two cores are then stacked coaxially and the bias and signal windings are wound on the pair as a unit. To minimize transformer effect between the output and the other windings, the two components of the output winding are matched and the cores stacked so that these two windings have the minimum mutual coupling.

Circuit Theory

The impedance which the modulator output coil exhibits in the series resonant circuit of the oscillator can be expressed as:

$$z = \frac{e}{i} = R_L + j\omega L \tag{19}$$

where: e is defined as the a-c voltage at the coil terminals.

i is defined as the a-c current in the winding.

R_L is defined as the total loss resistance of the coil.

ωL is defined as the lossless reactive component of z .

The impedance z varies as a function of modulator input signal. Consideration of Equations (18) and (19) leads to the conclusion that oscillator frequency, ω, is a function of z. The object of the following analysis is to define the relationship between oscillator frequency, ω, and z. Since the resistance, R_L, in Equation (19) is defined as the total loss resistance, this implies that the total losses in the modulator output coil are

$$W_T = I^2 R_L \tag{20}$$

where: I is the rms current in the winding.

The above losses can be divided into two groups as follows:

A. Losses in the winding
   1. Copper losses (d-c)
   2. Eddy current losses (a-c)
   3. Dielectric losses in the shunt capacitance in the windings

B. Losses in the core material
   1. Eddy current losses
   2. Hysteresis losses
   3. Residual losses

At the standard subcarrier oscillator frequencies (1 kc to 70 kc) and the a-c voltage and current levels used in the modulator output winding, the d-c copper losses exceed the total of all other winding losses by a factor of 10 or greater. In this analyses, therefore, the winding loss resistance will be assumed constant over the bandwidth of any particular subcarrier oscillator. With this assumption, the only variable components of R_L are the core material losses.

The winding loss component of R_L is designated R_w; the core material loss component, R_m. The component, R_m, is obviously the sum of the equivalent eddy current loss resistance, R_e, the equivalent hysteresis loss resistance, R_h, and the equivalent residual loss resistance, R_r, 5.

$$R_L = R + R_m \tag{21}$$

$$R_m \doteq R_e + R_h + R_r \tag{22}$$

where: $R_e = \epsilon\mu f^2 L$ (23)

$R_h = a\mu B m f L$ (24)

$R_r = c\mu f L$ (25)

and: ϵ, a, and c are constants of the core material

ϵ is the eddy current loss coefficient

a is the hysteresis loss coefficient

c is the residual loss coefficient

μ is the effective permeability of the core material

f is the frequency in cycles per second

L is the coil inductance

B_m is the maximum (peak-to-peak) magnetic flux density in the core material during operation

Equations (22), (23), (24), and (25) are assumed to be valid approximations at frequencies where the material Q, (designated Q_m),

$$Q_m = \frac{\omega L}{R_m} \tag{26}$$

is greater than 10. In ferrite core materials a decrease in Q_m to a value less than 10 as a result of increasing frequency, is accompanied by an increase in rate of change of the residual loss resistance. When this occurs, the coefficient c in Equation (25) becomes frequency dependent. The subcarrier oscillator frequencies are well below the frequency where c becomes variable in the ferrite core material used in the modulator.

At low flux densities, the hysteresis loss resistance varies linearly with the maximum flux density, B_m, as indicated in Equation (24). If the frequency is held constant in the subcarrier oscillator frequency range, and the a-c flux density, B_m, is increased steadily, a point will be reached where the relationships described in Equation (24) no longer apply. From this point, further increase in B_m produces a corresponding increase in hysteresis coefficient, a.

The L in Equation (19) is a function of the permeability of the core material.

$$L = L_o\mu \tag{27}$$

where: μ is the permeability of the core material

L_o is a constant depending upon the physical configurations of the core material and winding

The permeability μ is often represented as simply the ratio of magnetic induction to the applied , magnetizing force, or:

$$\mu = \frac{B}{H} \tag{28}$$

where: B is the magnetic induction or the magnetic flux per unit area of the core

H is the magnetizing force per unit length or the magnetic field intensity in the core material

Refer to Figure 6.

The magnetic field intensity is a linear function of the current in the winding and is expressed as:

$$H = \frac{4\pi Ni}{10\sum \ell_i} \qquad \text{(oersteds)} \tag{29}$$

where: N is the number of turns in the winding

ℓ_i is the mean length of the i^{th} flux path in centimeters

i is the current, in amperes, in the winding

The magnetic flux density in the core material is proportional to the voltage induced in the winding and varies inversely with the frequency of the current producing the magnetic field.

$$B = \frac{10^8 \, e_L}{\omega N \sum A_i} \qquad \text{(gauss)} \tag{30}$$

where: ω is the angular frequency of I

N is the number of turns in the winding

A_i is the cross sectional area in cm^2 of the i^{th} flux path

e_L is the induced voltage. This is the purely inductive component of the voltage appearing at the winding terminals

Rewriting Equation (28) and substituting the expressions for H and B in Equations (29) and (30), respectively:

$$\mu = \frac{B}{H} = \frac{1}{\omega} \left[\frac{10^9}{4\pi N^2} \sum \frac{\ell_i}{A_i} \right] \left[\frac{e_L}{i} \right] \tag{31}$$

Assume that the core material is temporarily removed without altering the flux distribution. The permeability becomes unity (the permeability of air). Using Equations (27) and (31), an expression can be derived for the constant, L_o. From the definition of e_L above:

$$e_L = \omega L i \tag{32}$$

and:

$$\frac{L}{L_o} = \frac{1}{\omega}\left[\frac{10^9}{4\pi N^2}\sum\frac{\ell_i}{A_i}\right]\left[\frac{L i}{i}\right] \tag{33}$$

or:

$$L_o = 4\pi N^2 10^{-9}\sum\frac{A_i}{\ell_i} \tag{34}$$

It is apparent that L_o is a constant for any particular modulator configuration.

The previous definition of permeability is based upon the assumption that the core material is in the presence of an alternating magnetic field only. If, in addition to the alternating field, a unidirectional polarizing field, H_b, is introduced, the magnetic flux density in the core material is changed by the presence of the polarizing field. When a d-c field, H_b, is thus superposed upon an a-c field, ΔH, the resulting permeability of the core material is the ratio of the cyclically changing induction, ΔB, to the cyclically changing field strength, ΔH, and is, by definition, the incremental permeability, μ_Δ. Refer to Figure 7. A d-c field, H_b, is used in the variable inductance modulator to control the incremental permeability of the core material. The inductance of the modulator output winding is proportional to the incremental permeability of the core material in precisely the same sense as that previously described by Equation (27). Therefore,

$$L = L_o \mu_\Delta \tag{35}$$

$$\mu_\Delta = \frac{\Delta B}{\Delta H} = \left[\frac{1}{L_o}\right]\left[\frac{e_L}{i}\right] \tag{36}$$

where: i is the a-c current in the modulator output winding.

e_L is voltage induced in the modulator output winding.

Again, it is necessary to state that e_L is the purely inductive component of the voltage appearing at the terminals of the modulator output winding. Since this voltage component cannot be measured directly, a more useful equation is obtained if μ_Δ is expressed in terms of the a-c voltage at the terminals of the modulator output winding. If the Q of the output winding is expressed as

$$Q_L = \frac{\omega L}{R_L} \tag{37}$$

the inductive component of the voltage e at the modulator output terminals is

$$e_L = \left[\frac{Q_L}{1 + j\,Q_L}\right] e \tag{38}$$

Using Equation (38), μ_Δ in terms of e and i is:

$$\mu_\Delta = \left[\frac{1}{L_o}\right]\left[\frac{Q_L}{1 + jQ_L}\right]\left[\frac{e}{i}\right] \tag{39}$$

or, from the definition of z in Equation (19)

$$\mu_\Delta = \left[\frac{z}{L_o}\right]\left[\frac{Q_L}{1 + jQ_L}\right] \tag{40}$$

Equation (40) illustrates the fundamental relationship between the magnetic properties of the core material, i.e., μ_Δ , and the electrical parameters associated with the modulator output winding. If the expression for μ_Δ in Equation (40) is substituted into Equation (35), an equation for oscillator frequency, ω , in terms of z and Q_L results.

$$\omega = \left[\frac{z}{L}\right]\left[\frac{Q_L}{1 + jQ_L}\right] \tag{41}$$

CRITERIA FOR LINEAR OPERATION

Definition of Linearity

At this point equations have been derived expressing oscillator frequency in terms of the oscillator equivalent series R, L, and C, Equations (18) and (19). Equation (41) expresses oscillator frequency in terms of the impedance of the modulator output winding. In order to use these equations in the derivation of an expression for linear modulation, the term "linear operation" must first be defined as it applies to this circuit.

The oscillator center frequency (RDB channel frequency) is obtained with no-signal or null-signal conditions in the modulator. For these conditions, the impedance of the modulator output coil is a function of the polarizing field produced by d-c current flow in the bias winding. When a signal is applied to the modulator to shift the oscillator frequency, current flows in the signal winding, changing the magnitude of the polarizing field acting on the core material. The change in polarizing field results in a change in impedance of the modulator output coil, which produces a corresponding change in oscillator frequency. The IRIG standard bandwidths for FM/FM subcarrier channels is ±7.5% for all standard channels, and ±15% for the special wide-band channels in the 22 KC to 70 KC range. Taking these facts into consideration, linear operation is defined as follows:

The relationship between the oscillator frequency and the magnitude of the modulating signal can be represented as a point on a single straight line at any frequency within the previously defined bandwidth of the oscillator.

This definition stated mathematically is:

$$\omega = K' \left| I_b + i_s \right| \quad , \quad \omega - \Delta\omega \leq \omega \leq \omega + \Delta\omega \tag{42}$$

Where ω is the oscillator frequency

$\Delta\omega$ is 7.5% ω for standard bandwidth channels and 15%ω for wide bandwidth channels.

K' is a constant.

I_b is the d-c bias current.

i_s is the instantaneous signal current.

$\left| I_b + i_s \right|$ is the effective magnitude of the modulating signal.

To simplify further derivations, the quantity $\left| I_b + i_s \right|$ will be represented by the symbol I_e. Rewriting Equation (42) using this notation

$$\omega = K' I_e \quad , \quad \omega - \Delta\omega \leq \omega \leq \omega + \Delta\omega \tag{43}$$

Linear Operation

The Q of the oscillator equivalent series R, L, C circuit is given by

$$Q = \frac{\omega L}{R} \tag{44}$$

in which R is the total resistance in the equivalent R, L, C circuit.

Equation (19) rewritten in terms of L and Q becomes

$$\omega = \frac{1}{\sqrt{L}} \left[\frac{4 K Q^2}{1 + 4 Q^2} \right]^{\frac{1}{2}} \tag{45}$$

or in terms of R and Q,

$$\omega = \frac{1}{R} \left[\frac{4 K Q}{1 + 4 Q^2} \right] \tag{46}$$

Using the definition of Q_L in Equation (37), Equation (41) can be rewritten in terms of L, Q_L and the magnitude of z as

$$\omega = \frac{|z|}{L} \left[\frac{Q_L^2}{1 + Q_L^2}\right]^{\frac{1}{2}} \tag{47}$$

Equations (45), (46), and (47) constitute a system of equations relating oscillator frequency to circuit parameters. By substituting Equation (43) into the above system, the relationships between I_e and z , R, L, Q and Q_L are thereby defined for linear operation, i.e.,

$$I_e = \frac{1}{K'\sqrt{L}} \left[\frac{4KQ^2}{1 + 4Q^2}\right]^{\frac{1}{2}} \tag{48}$$

$$I_e = \frac{1}{K'R} \left[\frac{4KQ}{1 + 4Q^2}\right] \tag{49}$$

$$I_e = \frac{z}{K'L} \left[\frac{Q_L^2}{1 + Q_L^2}\right]^{\frac{1}{2}} \tag{50}$$

Referring to the definitions of R, Q and Q_L the following relationships are apparent:

$$\omega L = R_L Q_L = RQ = (R_E + R_L)\, Q \tag{51}$$

If $R_L \gg R_E$, $Q \doteq Q_L$. This condition must be met in the design of the oscillator circircuit in order to minimize harmonic distortion in the oscillator output.

If an operating region exists in which the coefficients of the Q terms in Equations (48), (49) and (50) are linearly related, this implies that Q must be constant in this region. If $R_L \gg R_E$, $Q \doteq Q_L$, every point in the constant Q region represents a solution to the system of Equations (48), (49) and (50). Experimental data has shown that the constant Q region does exist. At every point within the constant Q region the oscillator frequency maintains a linear relationship to the magnitude of modulator signal. By selecting an operating point well within the region, linear operation is obtained over the required bandwidth of the oscillator. Refer to Figure 8.

The constant Q requirement for linear operation leads to a method of selecting a core material for the design of a variable inductance modulator. Refer to Equation (26) which defines Q_m. The relationship between Q_m and the Q of the oscillator equivalent R, L, C series resonant circuit is:

$$\omega L = Q_m R_m = QR = Q(R_E + R_w + R_m) \tag{52}$$

It has been shown experimentally that the existence of a constant Q_m region in a given core material implies that there exists a constant Q region in a practical modulator in which that core material is used. Refer to Figure 9. Although the two regions do not necessarily coincide at the boundaries, they intersect in all the core materials which have been investigated. Furthermore, the size of the constant Q_m region is similar to the size of the constant Q region.

Referring again to Equations (48), (49) and (50), it is apparent that linear dependence of the Q factor coefficients and constant Q are not mathematically unique boundary conditions for simultaneous solution of these equations. A unique solution requires the existence of at least three more independent relationships between the variables. Perhaps a more precise analysis of the oscillator circuit and the loss characteristics of the modulator core material would produce the relationships required to prove that the previously described boundary conditions do lead to a unique solution of the system. Experimentally, linear operation has been obtained only in the constant Q regions.

Temperature Stability

By selecting an operating point well inside the experimentally determined boundaries of the constant Q region, the change in core parameters over the temperature range of -30°C to +80°C does not move the operating point outside the region. The change in the core parameters does, however, affect the incremental permeability and loss resistance of the material. This results in corresponding changes in impedance of the modulator output winding which produce oscillator frequency drift. The core material incremental permeability and loss resistance have been held essentially constant over the above temperature range by controlling the a-c field, ΔH, so that it varies with temperature in such a manner as to compensate for the changes in parameters indicated above. The most effective means of accomplishing this involves the use of a thermistor temperature compensating circuit which causes the magnitude of the a-c current to vary as a function of temperature. By controlling the magnitude of the a-c current, the a-c field is similarly controlled.

Non-Linear Operation

Some experimental effort has been expended investigating the effect of using damping techniques to alter the flux distribution in the core material. The results of these investigations show that the boundary conditions for linear operation were, in some instances, radically changed when these techniques were employed. This tends to indicate that the magnetic modulator can be used to produce practically any response characteristic which may be desired simply by controlling the flux distribution in the core material.

PERFORMANCE

Several laboratory prototypes of the variable inductance modulated oscillator circuit have been constructed. The ferrite core material used in the modulators of these units is Ferramic 03 recently developed by General Ceramics Corporation.

The operating points for the laboratory prototypes have been selected well inside the constant Q region previously described. The linearities obtained in the prototypes have been consistently better than one percent of bandwidth deviation from a straight line. Modulator sensitivity is uniform for the prototypes tested.

A thermistor temperature compensating network has been incorporated in the oscillator to minimize frequency drift. The temperature compensating network adjusts the modulator a-c field strength to compensate for changes in core material parameters. Frequency drift has been held to within ±3% of bandwidth over the -30°C to 80°C temperature range. In the prototypes tested, the change in linearity over the above temperature range was less than 1% of bandwidth deviation from a straight line. The change in sensitivity was also less than 1% of bandwidth over the temperature range. It appears that no significant variations from the above performance criteria will be encountered in production.

APPLICATION

The immediate application of the variable inductance modulated oscillator described in this paper is in a complete new line of miniaturized FM/FM subcarrier oscillators. The circuit shown in Figure 10 is being used as a basic component in a transistorized current-controlled oscillator (TCCO), a transistorized voltage-controlled oscillator (TVCO), and a transistorized thermocouple-controlled oscillator (TTCO). Block diagrams of the complete subcarrier oscillator units are shown in Figure 11.

The TCCO includes a temperature-stabilized d-c differential amplifier to convert the low-level output of a resistive bridge transducer into a signal current of suitable magnitude for the variable inductance modulator. The TCCO operates from a regulated, 12-volt d-c power supply which also supplies d-c excitation to the resistive bridge transducer. This feature decreases overall power requirements and provides increased stability in the amplifier.

The TVCO also uses a d-c differential amplifier similar in design to that used in the TCCO. The differential amplifier is temperature-stabilized for -30°C to 80°C operation and features 0.3 megohm input impedance.

The TTCO input circuit is a single low impedance winding in the variable inductance modulator. This provides extremely good stability, since the need for an amplifier has been eliminated. The signal winding in the modulator is floating which allows for grounding either side of the thermocouple.

In addition to the applications enumerated above, a TVCO with logarithmic frequency response is being designed using the basic variable inductance modulated oscillator.

The possible applications of the variable inductance modulation principle are almost unlimited in the field of instrumentation and remote control. The outstanding advantages which this type of modulation offers over others are its comparative simplicity, flexibility and inherent reliability.

CONCLUSIONS

The inherent non-linearity of a variable inductance modulated oscillator has, until recently, prevented its use as a subcarrier oscillator in FM/FM telemetry systems. The development of a method for obtaining linear operation of a variable inductance modulated oscillator has led to its application in the design of a complete line of subcarrier oscillators. Linear operation is obtained in an operating region where the Q of the oscillator resonant circuit is constant over the bandwidth of the subcarrier oscillator. Experimental results obtained using the oscillator circuit described in this paper indicate that the above criteria for linear operation requires the existence of a constant Q_m region in the characteristics of the modulator core material. The larger the constant Q_m region, the less critical is the design of the modulator.

A simple and effective method for temperature stabilizing the variable inductance modulated oscillator involves controlling the magnitude of the a-c field of the modulator so that it varies in such a manner as to compensate for changes in core material parameters with temperature.

REFERENCES

1. Analysis and Performance Characteristics of Transistorized Subcarrier Oscillator Circuits for Airborne Telemetering, M. M. Wilkinson. IRE Proceedings of the 1958 National Symposium on Telemetering, paper 2.2
2. A Transistorized Current - Controlled Oscillator for DC Excited Strain Gage Applications, C. E. Land. Proceedings 1958 National Telemetering Conference, pp. 215-26.
3. Ferromagnetism (book), R. M. Bozorth. D. Van Nostrand Company, Inc., New York, 1951.
4. The Physics of Magnetic Materials, R. M. Bozorth, Electrical Engineering, Vol. 75, February 1956, pp. 134-40.
5. Magnetic Measurements at Low Flux Densities Using the Alternating Current Bridge, V. E. Legg. Bell System Technical Journal, Vol. 16, 1936, pp. 39-62.
6. Analysis of the Measurements on Magnetic Ferrites, C. D. Owens, Proceedings IRE, Vol. 41, March 1953, p. 359.

ACKNOWLEDGEMENTS

The author wishes to acknowledge the guidance and assistance of Mr. George E. Reis in the mathematical derivations and in the preparation and editing of this paper. The author also wishes to acknowledge the contributions of Mr. Reuben H. Gablehouse, Mr. John B. Noe and Mr. Pete Hernandez to the design and development of the circuits described in this paper.

APPENDIX A

Definitions of Symbols

r_e Instantaneous value of oscillator transistor emitter resistance (Figure 2).

r_b Instantaneous value of oscillator transistor base resistance (Figure 2).

r_c Instantaneous value of oscillator transistor collector resistance (Figure 2).

V_{BE} Instantaneous base to emitter voltage (Figure 2).

V_{CE} Instantaneous collector to emitter voltage (Figure 2).

Assuming the transistor ideal switch analogy, the following symbols pertain to the "off" switching condition (Figure 3A):

R_1 The equivalent resonant circuit series resistance.

C_1 The equivalent resonant circuit series capacitance.

ω_1 The oscillator frequency (natural frequency of the equivalent series resonant circuit).

Assuming the transistor ideal switch analogy, the following symbols pertain to the "on" switching condition (Figure 3B):

R_2 The equivalent resonant circuit series resistance.

C_2 The equivalent resonant circuit series capacitance.

ω_2 The oscillator frequency (natural frequency of the equivalent series resonant circuit).

The following symbols pertain to the true equivalent series resonant circuit of the oscillator (Figure 4):

R The true equivalent circuit series resistance.

C The true equivalent circuit series capacitance.

ω The actual oscillator frequency (the natural frequency of the true equivalent R, L, C series resonant circuit).

R_E The total component of R not attributable to the inductor.

z The impedance of the modulator output winding ($R_L + j\omega L$).

R_L The total loss resistance of the modulator output winding.

R_w The component of R_L attributable to the winding losses.

R_m The component of R_L attributable to the core material losses.

R_e The component of core material loss resistance, R_m, due to eddy current losses.

R_h The component of core material loss resistance, R_m, due to hysteresis losses.

R_r The component of core material loss resistance, R_m, due to residual losses.

ϵ	Eddy current loss coefficient.
h	Hysteresis loss coefficient.
c	Residual loss coefficient.
W_T	Total losses attributable to the modulator output coil.
μ	The permeability of the core material
B	Magnetic induction or magnetic flux per unit of core cross sectional area.
H	Magnetizing force per unit length of core.
e	The a-c voltage at the terminals of the modulator output winding.
e_L	The purely inductive component of e.
i	The a-c current in the modulator output winding.
A_i	Cross sectional area in cm^2 of the i^{th} flux path.
ℓ_i	Length in cm of the i^{th} flux path.
L	The inductance of the modulator output winding.
L_o	A constant relating L to μ (Equation (27)).
μ_Δ	The incremental permeability of the core material. The permeability exhibited by the core material in the presence of both a-c and d-c fields.
ΔH	The cyclically changing (a-c) field superposed on a d-c polarizing field.
ΔB	The cyclically changing (a-c) induction or flux density due to the presence of ΔH.
H_b	The notation used for field intensity of a d-c polarizing or biasing field.
B_b	The effective bias flux density depending upon the magnitudes of both H_b and ΔH.
Q	$\left(\frac{\omega L}{R}\right)$ Quality factor of oscillator equivalent series resonant R, L, C, circuit.
Q_L	$\left(\frac{\omega L}{R_L}\right)$ Quality factor of modulator output coil.
Q_m	$\left(\frac{\omega L}{R_m}\right)$ Quality factor of modulator core material.
I_b	Modulator d-c bias current.
i_s	Modulator instantaneous signal current.
I_e	$\lvert I_b + i_s \rvert$ Effective magnitude of the modulating signal.
$\triangleq$	Equals, by definition.
$\doteq$	Equals, approximately.

APPENDIX B

Derivation of R_c and C_1 for the "OFF" or Non-conducting State of the Oscillator Transistor

Refer to Figures 2 and 3A. Let the equivalent impedance of the C1, C2, and R2 combination (for the transistor "off" state) be Z_c. Then,

$$Z_c = R_c + j X_c \qquad (1)$$

where:

$$X_c = \frac{1}{\omega_1 C_1}$$

Therefore:

$$Z_c = \frac{(-j X_1)(R_2 - j X_2)}{R_2 - j(X_1 + X_2)} \qquad (2)$$

where:

$$X_1 = \frac{1}{\omega_1 C1}$$

$$X_2 = \frac{1}{\omega_1 C2}$$

Rationalizing Equation (2):

$$Z_c = \frac{R2X_1^2 - j\,(R2^2X_1 + X_1^2 X_2 + X_1X_2^2)}{R2^2 + (X_1 + X_2)^2}$$

$$Z_c = \left[\frac{R2\,X_1^2}{R2^2 + (X_1 + X_2)^2}\right] - j\left[\frac{R2^2X_1 + X_1X_2(X_1 + X_2)}{R2^2 + (X_1 + X_2)^2}\right] \qquad (3)$$

Equation (3) is in the same form as Equation (1), therefore:

$$R_c = \frac{R2\,X_1^2}{R2^2 + (X_1 + X_2)^2}$$

$$X_c = \frac{R2^2 X_1 + X_1 X_2 (X_1 + X_2)}{R2^2 + (X_1 + X_2)^2} \tag{5}$$

Rewriting Equations (4) and (5) in terms of ω_1, C1, and C2:

$$R_c = \frac{R2\, C2^2}{\omega_1^2\, C1^2\, C2^2\, R2^2 + (C1 + C2)^2} \tag{6}$$

$$X_c = \left[\frac{1}{\omega_1}\right]\left[\frac{\omega_1^2\, C1\, C2^2\, R2^2 + (C1 + C2)}{\omega_1^2\, C1^2\, C2^2\, R2^2 + (C1 + C2)^2}\right] \tag{7}$$

Since

$$X_c = \frac{1}{\omega_1 C_1}$$

$$C_1 = \frac{\omega_1^2\, C1^2\, C2^2\, R2^2 + (C1 + C2)^2}{\omega_1^2\, C1\, C2^2\, R2^2 + (C1 + C2)}$$

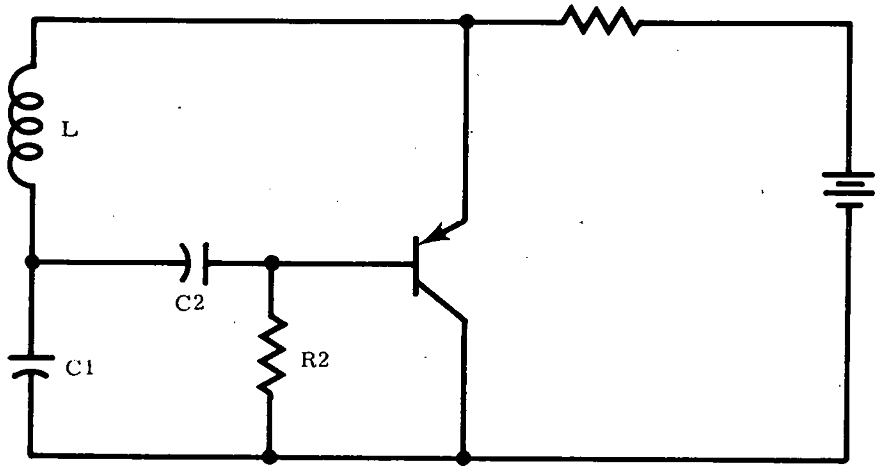

Figure 1

Oscillator Simplified Schematic

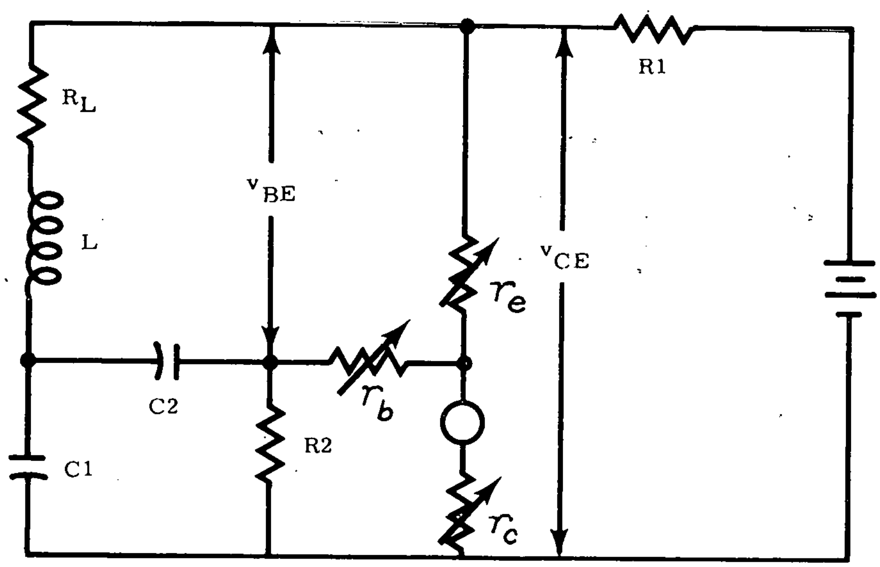

Figure 2

Oscillator Approximate Equivalent Circuit

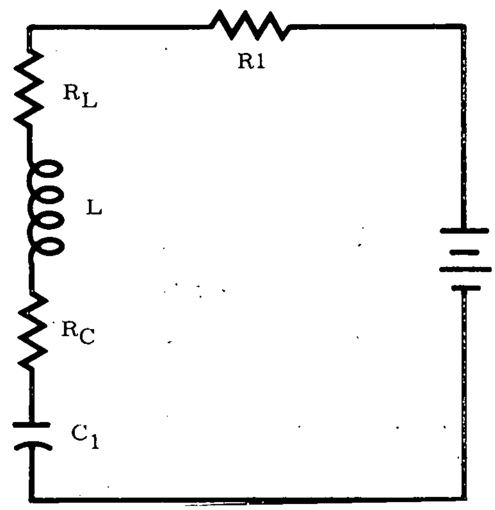

Figure 3A

Oscillator Approximate Equivalent Circuit for Transistor Non-Conducting Condition

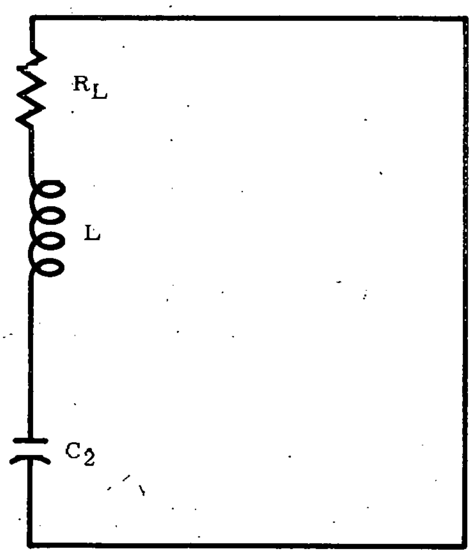

Figure 3B

Oscillator Approximate Equivalent Circuit for Transistor Conducting (Saturation) Condition

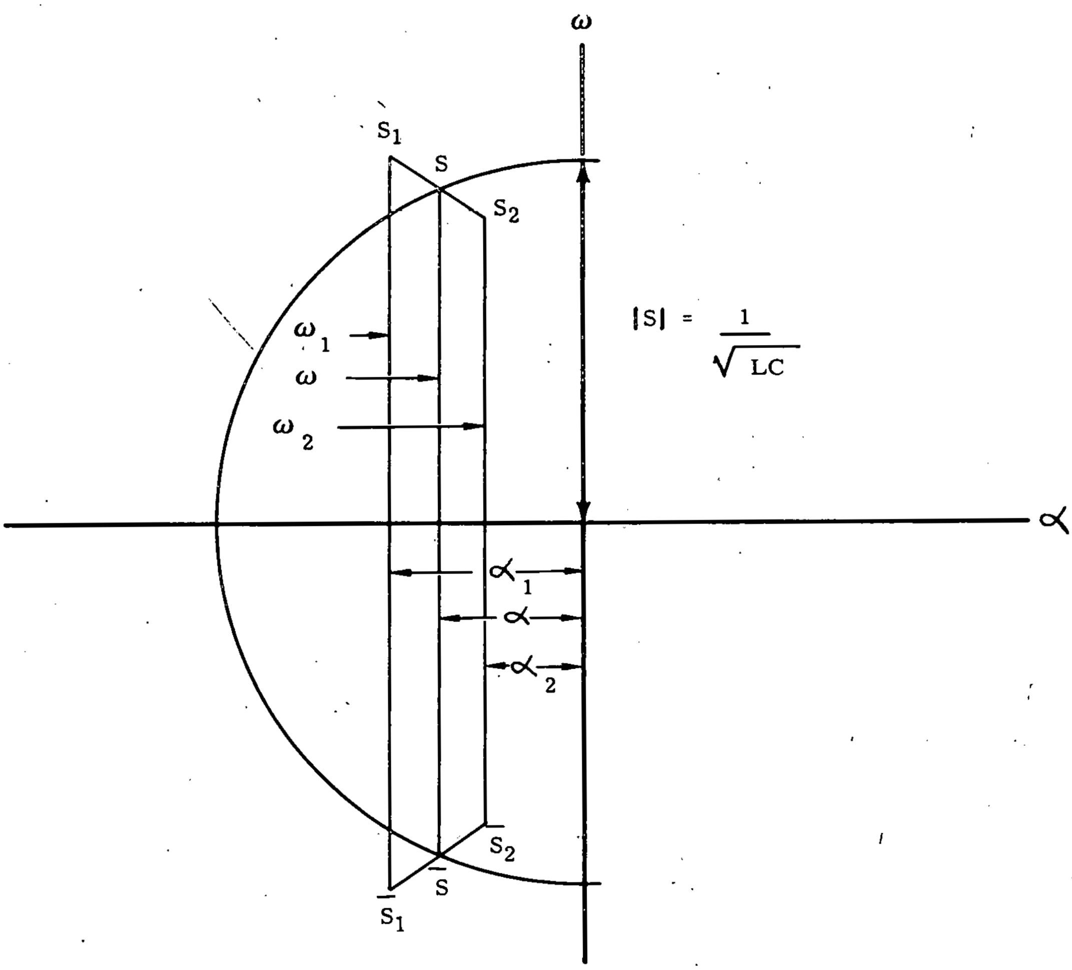

Figure 4

Complex Frequency Plane Representation Oscillator Equivalent Series Resonant Circuit

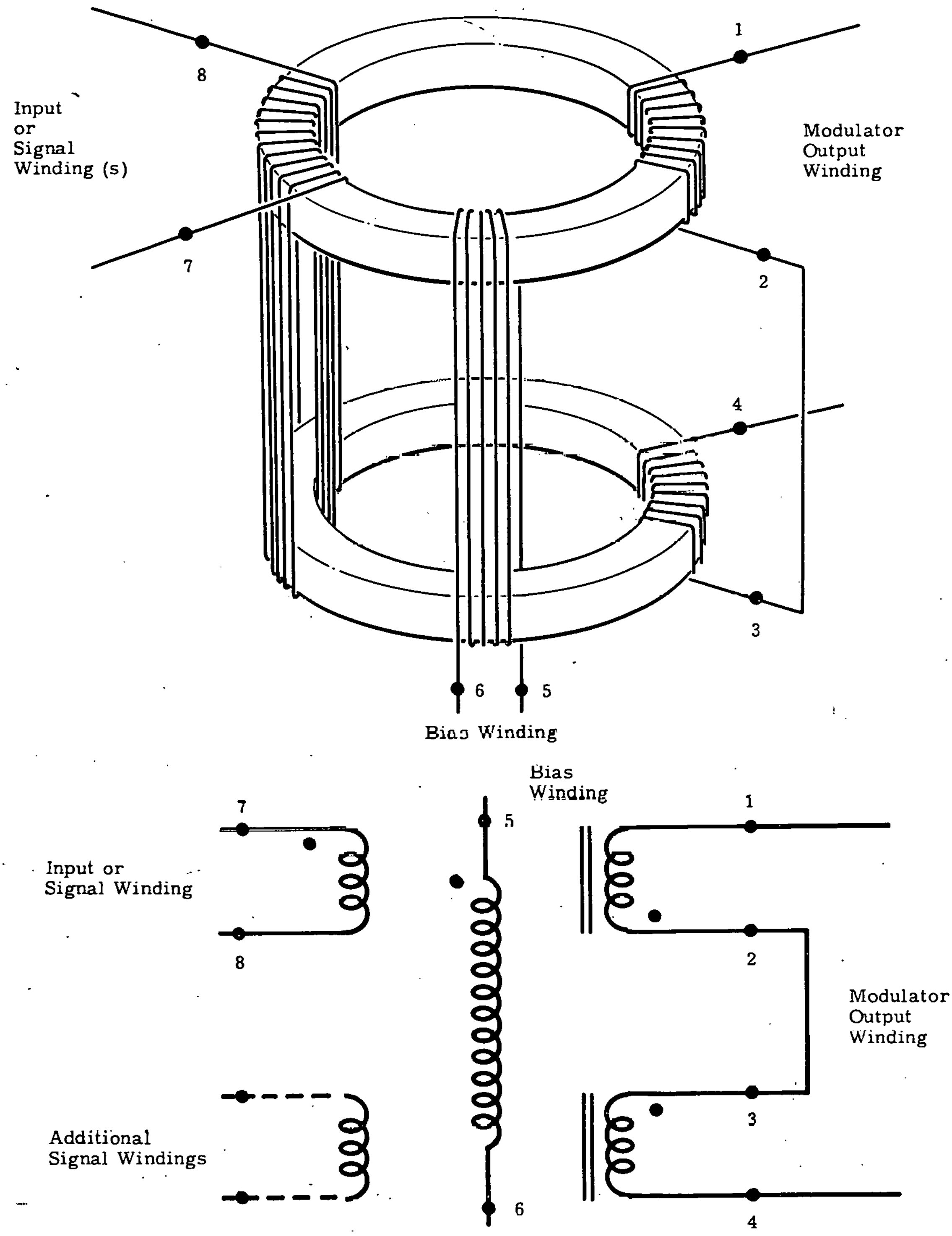

Figure 5

Modulator Construction Detail and Schematic Diagram

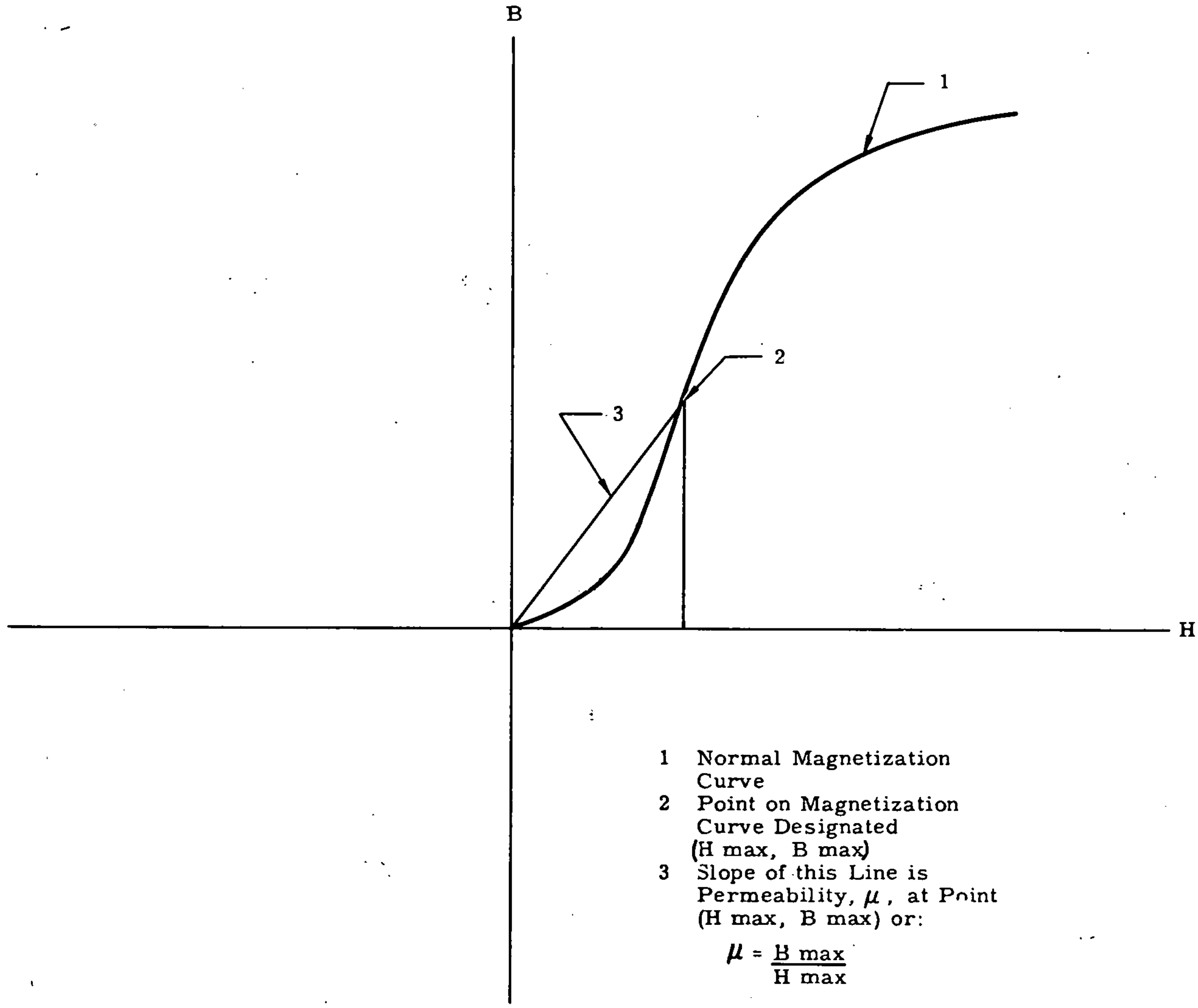

Figure 6

Definition of Permeability, μ

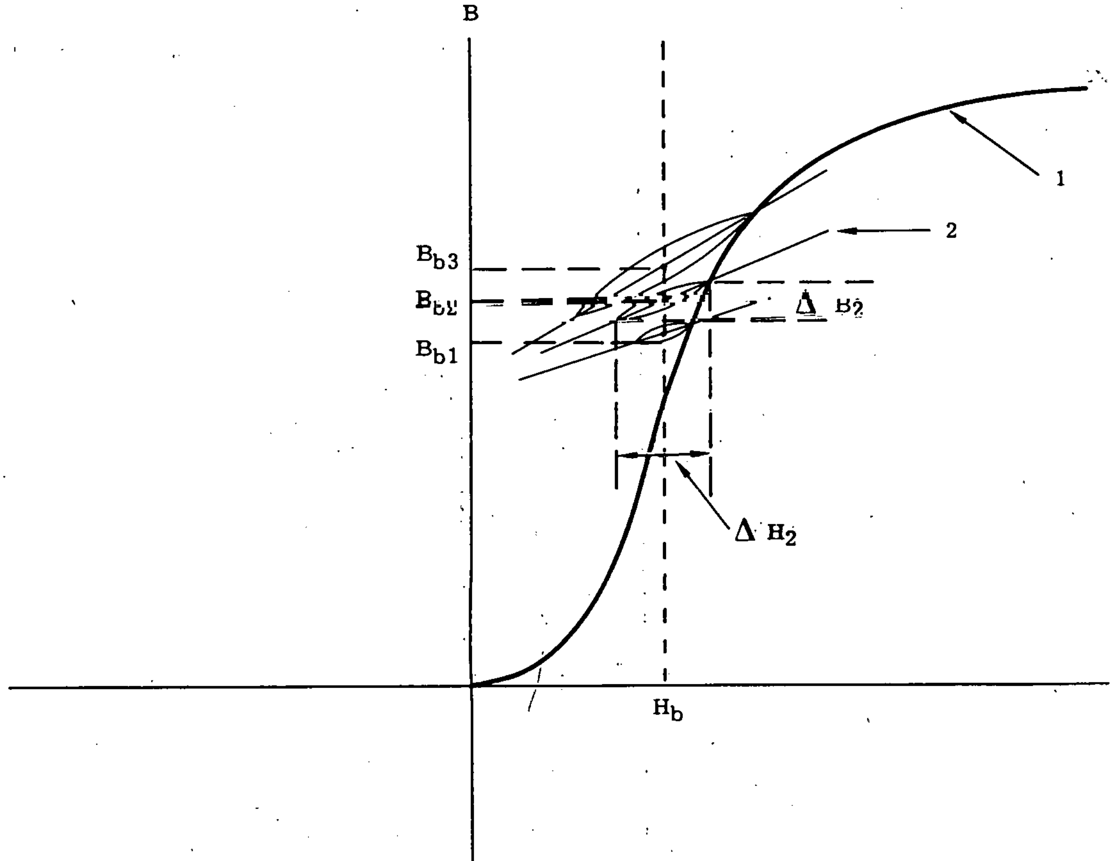

1 Normal Magnetization Curve

2 Slope of this Line is Incremental Permeability, $\mu\Delta$, at Point (H_b, B_{b2}), or:

$$\mu\Delta = \frac{\Delta B_2}{\Delta H_2}$$

Figure 7

Definition of Incremental Permeability, $\mu\Delta$

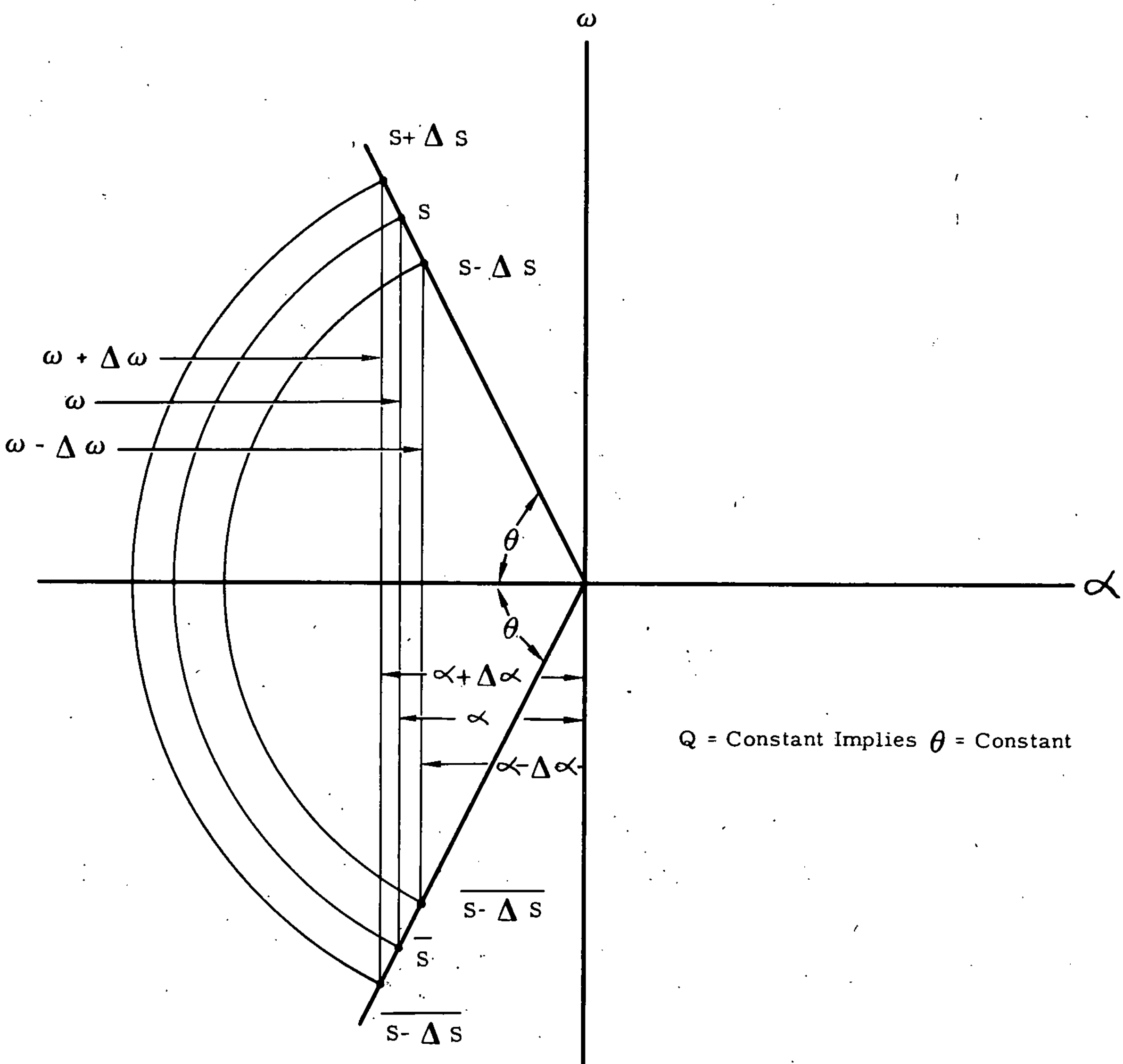

Figure 8

Linear Oscillator Operation Illustrated in S- Plane

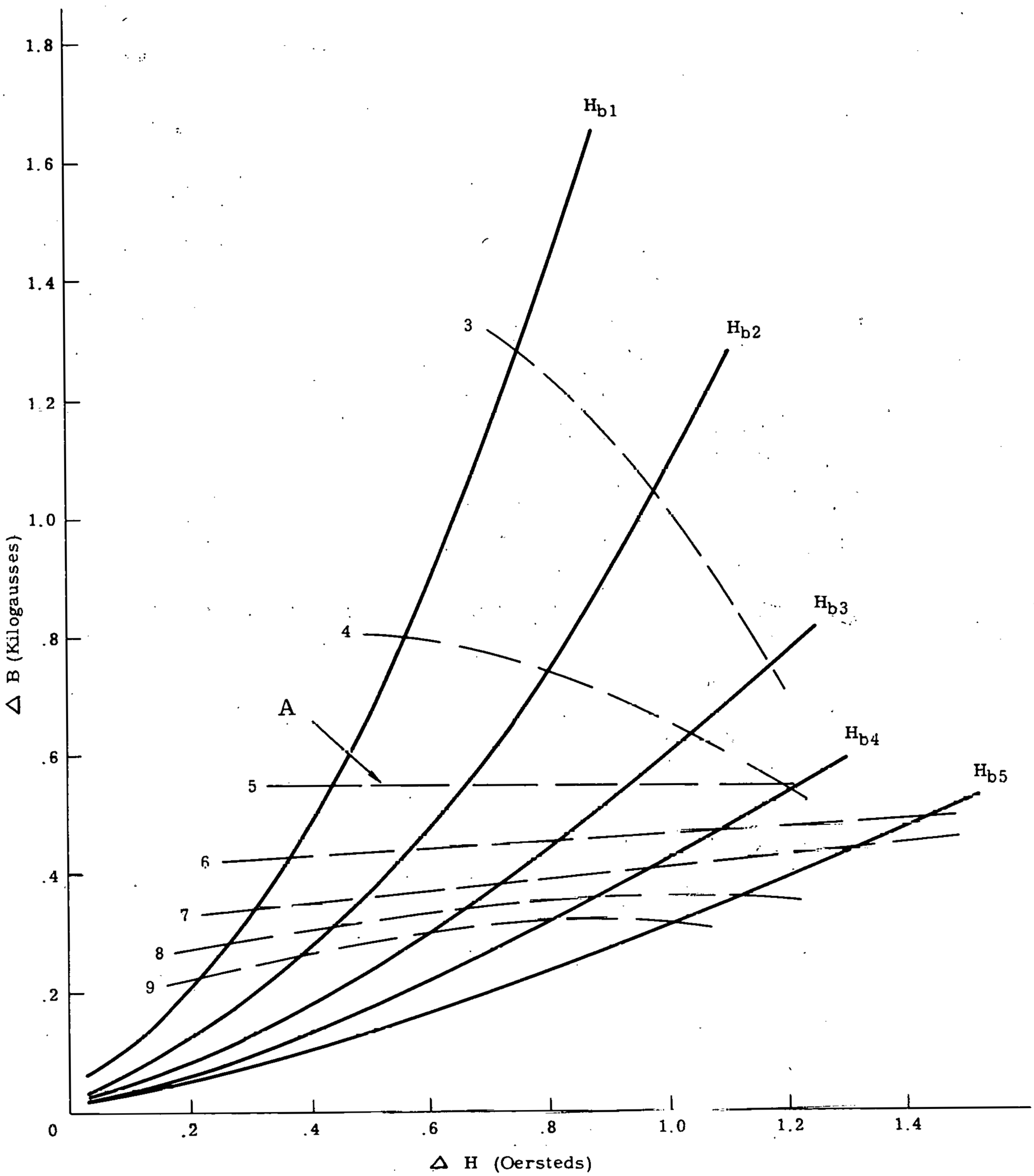

Figure 9

Characteristics of Ferramic 03 Material Showing Qm Contours.
A Designates Constant Qm Contour

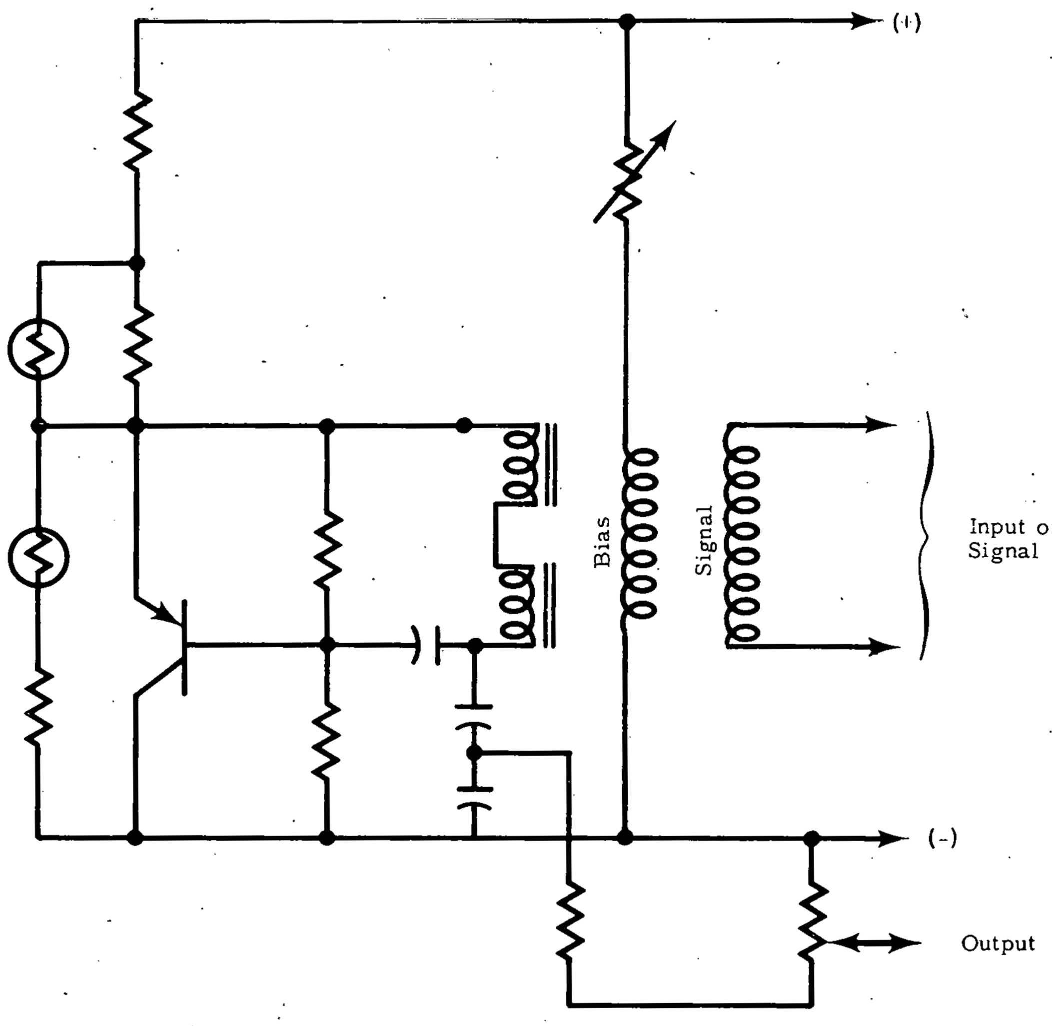

Figure 10

Oscillator Schematic Diagram

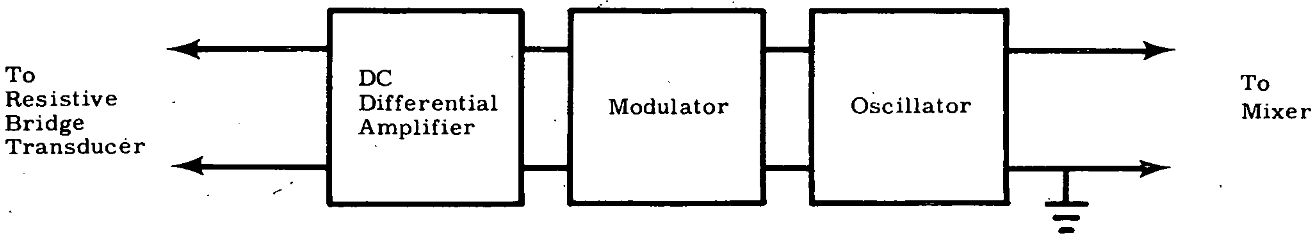

Figure 11A

Block Diagram, TCCO

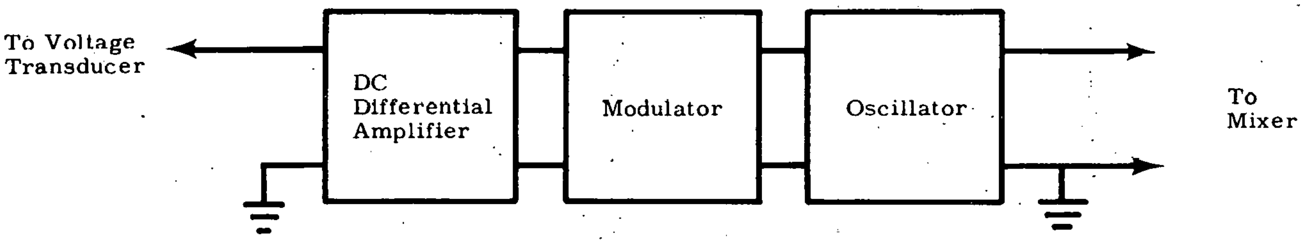

Figure 11B

Block Diagram, TVCO

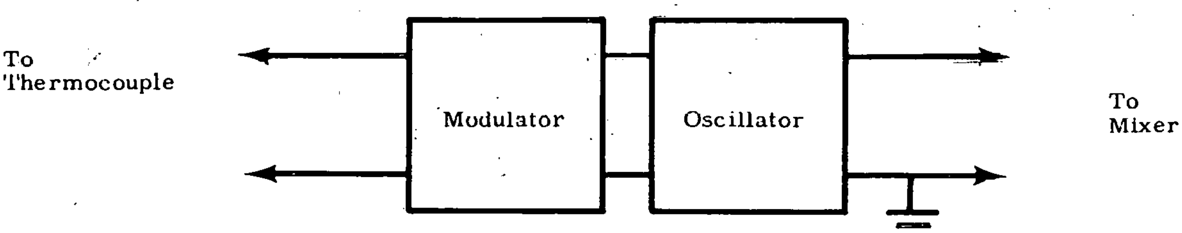

Figure 11C

Block Diagram, TTCO

TID 4500 (14th Ed.)

INSTRUMENTS

STANDARD DISTRIBUTION

	No. of Copies
Aberdeen Proving Ground	3
Aerojet-General Corporation	1
Aerojet-General, San Ramon (IOO-880)	1
Air Force Cambridge Research Center	1
Air Force Institute of Technology	1
AFPR, Boeing, Seattle	1
AFPR, Lockheed, Marietta	2
Air Force Special Weapons Center	2
ANP Project Office Convair, Fort Worth	2
Alco Products, Inc.	1
Argonne Cancer Research Hospital	1
Argonne National Laboratory	10
Armed Forces Special Weapons Project, Washington	1
Armed Services Technical Information Agency	5
Army Ballistic Missile Agency	1
Army Chemical Center	3
Army Signal Research and Development Laboratory	1
Atomic Bomb Casualty Commission	1
AEC Scientific Representative, Argentina	1
AEC Scientific Representative, Japan	1
Atomic Energy Commission, Washington (TL)	3
Atomics International	3
Babcock and Wilcox Company (NYOO-1940)	1
Battelle Memorial Institute	2
Bettis Plant	4
Brookhaven National Laboratory	4
Bureau of Medicine and Surgery	1
Bureau of Mines, Salt Lake City	1
Bureau of Ships (Code 1500)	1
Carnegie Institute of Technology	1
Chicago Operations Office	1
Chicago Patent Group	1
Columbia University (Failla)	1
Columbia University (Havens)	1
Combustion Engineering, Inc.	2
Convair-General Dynamics Corporation, San Diego	1
Defence Research Member	2
Department of the Army, G-2	2
Division of Raw Materials, Austin	1
Division of Raw Materials, Denver	1
Division of Raw Materials, Grants Branch	1
Division of Raw Materials, Salt Lake City	1
Division of Raw Materials, Washington	1
Dow Chemical Company (Rocky Flats)	1
duPont Company, Aiken	4
duPont Company, Wilmington	1
Edgerton, Germeshausen and Grier, Inc., Boston	1
Edgerton, Germeshausen and Grier, Inc., Las Vegas	1
Frankford Arsenal	1
General Electric Company (ANPD)	2
General Electric Company, Richland	4
General Nuclear Engineering Corporation	1
Gibbs and Cox, Inc.	1

Standard Distribution (cont)

	No. of Copies
Goodyear Atomic Corporation	1
Grand Junction Operations Office	1
Hawaii Marine Laboratory	1
Iowa State College	1
Jet Propulsion Laboratory	1
Knolls Atomic Power Laboratory	2
Los Alamos Scientific Laboratory	2
Lovelace Foundation	1
Mallinckrodt Chemical Works	1
Maritime Administration	1
Martin Company	1
Mound Laboratory	1
National Advisory Committee for Aeronautics, Cleveland	1
National Bureau of Standards	1
National Bureau of Standards (Library)	1
National Institutes of Health	1
National Lead Company of Ohio	1
Naval Medical Research Institute	1
Naval Research Laboratory	3
New Brunswick Area Office	1
New York Operations Office	2
Nuclear Development Corporation of America	1
Nuclear Metals, Inc.	1
Oak Ridge Institute of Nuclear Studies	1
Office of Naval Research	10
Office of Naval Research (Code 422)	1
Office of Ordnance Research	1
Office of the Surgeon General	1
Ordnance Materials Research Office	1
Ordnance Tank-Automotive Command	1
Patent Branch, Washington	1
Phillips Petroleum Company (NRTS)	4
Picatinny Arsenal	1
Power Reactor Development Company	1
Pratt and Whitney Aircraft Division	2
Princeton University (White)	1
Public Health Service	2
Public Health Service, Savannah	1
Sandia Corporation, Albuquerque	2
South Dakota School of Mines and Technology	1
Technical Research Group	1
Tennessee Valley Authority	1
The Surgeon General	1
Union Carbide Nuclear Company (ORGDP)	2
Union Carbide Nuclear Company (ORNL)	5
Union Carbide Nuclear Company (ORNL-Y-12)	1
Union Carbide Nuclear Company (Paducah Plant)	1
USAF Project RAND	1
U. S. Geological Survey, Denver	1
U. S. Geological Survey, Menlo Park	1
U. S. Geological Survey, Naval Gun Factory	1
U. S. Geological Survey, Washington	1
U. S. Naval Postgraduate School	1
U. S. Naval Radiological Defense Laboratory	2
U. S. Patent Office	1
UCLA Medical Research Laboratory	1
University of California Medical Center	1
University of California Radiation Laboratory, Berkeley	2

Standard Distribution (cont)

	No. of Copies
University of California Radiation Laboratory, Livermore	2
University of Chicago, USAF Radiation Laboratory	1
University of Puerto Rico	1
University of Rochester	1
University of Rochester (Marshak)	1
University of Utah	1
University of Washington (Geballe)	2
University of Washington (Rohde)	1
Vitro Engineering Division	1
Walter Reed Army Medical Center	1
Watertown Arsenal	1
Western Reserve University	1
Westinghouse Electric Corporation (Schafer)	1
Wright Air Development Center	11
Yankee Atomic Electric Company	1
Technical Information Service Extension	325
Office of Technical Services, Washington	100
	625

Issued by
Technical Information Division
Sandia Corporation
Albuquerque, New Mexico